J. Astrophys. Astr. (June 2017) 38:19
DOI 10.1007/s12036-017-9443-z

Metallicity of Sun-like G-stars that have Exoplanets

SHASHANKA R. GURUMATH[1,*], K. M. HIREMATH[2] and V. RAMASUBRAMANIAN[1]

[1]Department of Physics, School of Advanced Sciences (SAS), VIT University, Vellore 632 014, India.
[2]Indian Institute of Astrophysics, Bangalore 560 034, India.
*Corresponding author. E-mail: shashankgurumath@yahoo.in

MS received 10 June 2016; accepted 20 April 2017; published online 19 June 2017

Abstract. By considering the physical and orbital characteristics of G type stars and their exoplanets, we examine the association between stellar mass and its metallicity that follows a power law. Similar relationship is also obtained in case of single and multiplanetary stellar systems suggesting that, Sun′s present mass is about 1% higher than the estimated value for its metallicity. Further, for all the stellar systems with exoplanets, association between the planetary mass and the stellar metallicity is investigated, that suggests planetary mass is independent of stellar metallicity. Interestingly, in case of multiplanetary systems, planetary mass is linearly dependent on the stellar absolute metallicity, that suggests, metal rich stars produce massive ($\geq$1 Jupiter mass) planets compared to metal poor stars. This study also suggests that there is a solar system planetary missing mass of $\sim$0.8 Jupiter mass. It is argued that probably 80% of missing mass is accreted onto the Sun and about 20% of missing mass might have been blown off to the outer solar system (beyond the present Kuiper belt) during early history of solar system formation. We find that, in case of single planetary systems, planetary mass is independent of stellar metallicity with an implication of their non-origin in the host star's protoplanetary disk and probably are captured from the space. Final investigation of dependency of the orbital distances of planets on the host stars metallicity reveals that inward migration of planets is dominant in case of single planetary systems supporting the result that most of the planets in single planetary systems are captured from the space.

Keywords. Sun: evolution—stars: chemical abundances—stars: metallicity—stars: planetary systems.

1. Introduction

Birth of a stellar system takes place in the nebula which consists of gas and dust particles that are basic ingredients for the formation of stars and planets. The amount of gas, dust particles, chemical composition or metallicity of the nebula play a significant role in the formation of planetary system (Ksanfomality 2004; Moriarty *et al.* 2014; Reboussin *et al.* 2015). Hence, study of stellar metallicity and its relation with different physical characteristics of host stars and their planets may lead to better understanding of the planetary system formation. Before the era of discovery of exoplanets, many planetary models concentrated mainly on the genesis of solar system formation. The discovery of many exoplanetary systems (Boss *et al.* 2010; Lammer *et al.* 2010; Dressing & Charbonneau 2015) led to many new models (de Wit & Seager 2013; Kerr *et al.* 2015) that further improved the knowledge of physics of planetary formation. In early studies, it was found that the stars with planets have a higher metallicity than the stars without planets (Gonzalez *et al.* 2001b). However, low mass giant stars ($\leq 1.5 M_{\odot}$) with planets did not show any difference in their metallicity when compared with giant stars without planets (Maldonado *et al.* 2013).

Previous studies (Gonzalez 2000; Santos *et al.* 2000) indicated that the detection of gas giants or hot Jupiters are more around the metal-rich stars than the metal-poor stars. That means, formation of giant planet is low around the metal-poor stars (Fischer & Valenti 2005). Mordasini *et al.* (2012) showed that occurrence rate and mass of giant planets depend on the thickness and timescale of protoplanetary disk. On the other hand, occurrence rate of terrestrial planets or low mass planets is independent of the host star's metallicity (Buchhave *et al.* 2014). One explanation for the high mass planets around the metal-rich stars is inward migration of planets during the early history of stellar system formation (Dawson & Murray-Clay 2013). Due to inward migration, high mass planets scatter the planetesimals

(or gas and dust particles) that are present in the protoplanetary disk. These scattered planetesimals most likely accrete on the host star's convective envelope as a 'pollution' and hence, increases the stars metallicity (Vauclair & Vauclair 2014). During early evolutionary stages, accreted mass mix deep inside a star, whereas, in later stages, accreted mass mix only in a shallow convective envelope. For example, the presence of ^{6}Li in the stellar system supports the accretion of planetary mass on the host star (Reddy *et al.* 2002; Santos *et al.* 2009; Mena *et al.* 2012). Hence, the effect of 'pollution' is one of the important factor that likely determines the final metallicity of host stars and, the massive planets near-by host star may be the reason for increase in the metallicity of host stars during the early history of stellar system formation.

Another explanation for high mass planets around metal-rich stars is the metal-rich nebula from which host stars and planets are formed (Gonzalez 2006). This implies that the metal-rich protoplanetary disk around a host star (Gonzalez 2003; Bean *et al.* 2006) provides more gas and dust particles for the planetary formation. Adibekyan *et al.* (2012) confirmed that the rate of planetary formation is high in the galactic-thick disk than in the galactic-thin disk. This study also suggests that when the iron metal content is less, other metals play a major role in the planetary formation. The metal-rich disk with high concentration of Si, Ca, Mg, Al, etc. provides a good platform for the planetary core formation (Bodaghee *et al.* 2003). In addition, formation of terrestrial planets cannot be neglected around the metal-rich stars (Wang & Fischer 2015), because, probability of formation of the solid core is high due to more number of dust particles in the disk, which eventually lead to solid planets that are within the snow line.

The volatile elements like carbon compounds and oxygen help in the formation of gaseous envelope or planetary atmospheres. Among various volatile materials, oxygen plays a major role in the planetary formation via ice accretion beyond the snow line and also by the oxides of Si, Mg, Al, Ca, etc. (Brugamyer *et al.* 2011). The silicate grains provide a good platform for the planetary formation and these grains with accretion of icy mantle may grow into gas giants. Interestingly, there is no significant difference in the abundance of [C/Fe] and [O/Fe] in stars with planets and stars without planets (Gonzalez *et al.* 2001b; Da Silva *et al.* 2011). Although contribution of these materials to metallicity of the host star is insignificant, their major role in planetary formation cannot be neglected.

With this brief introduction, the following are the aims of the present study: (i) from the information of metallicity of host stars that have exoplanets, we try to understand how the metal content of a stellar nebula might have affected the planetary formation, (ii) we examine whether single and multiplanetary systems have similar mechanism of planetary formation or not, and the role of host stars' metallicity in these mechanisms, (iii) an attempt is made to confirm whether our solar system is also governed by the same universal mechanism of planetary formation and, (iv) we investigate whether stellar metallicity [Fe/H] is affected by average galactic metallicity that in turn might have influenced the planetary formation. The plan of the present study is as follows: description of the data used and the analysis are presented in section 2. The results with a brief discussion are presented in section 3, followed by conclusions in section 4.

2. Data and analysis

In order to examine the role of metallicity in the planetary formation of Sun-like G stars, physical and orbital characteristics of exoplanets and their host stars of G type are considered from the website http://exoplanet.eu/catalog/all_fields/. Many previous studies make use of this catalog for understanding the physics of host stars, dynamics and atmospheres of their planets, etc. For example, estimation of metallicity of host stars (Lindgren *et al.* 2016), atmospheric (Walsh & Millar 2011) and orbital (Antoniadou & Voyatzis 2016) studies of exoplanets, etc. Hence, this data set is most reliable to get answers for our aims.

We consider 225 exoplanets that belong to 179 host stars. Out of 225 exoplanets, 139 are detected by radial velocity method and the remaining are detected by transit method. Among these, majority (148) of stars are single planetary hosts (only one planet for a star) and, 31 (with 77 planets) are multiplanetary hosts (more than one planet for a star). Although one can argue that single planetary hosts are due to limitations in detection techniques, at present it is not clear whether single planets are really single planets or this is due to limitations of the detection. It is also not clear, due to limitations of observational detection, how much percentage of the data sample is due to the single planet. However, in this study we assume that these are single planets.

With the present precision of detection techniques, number of planets that are detected from space- and ground-based missions are given in Table 1. From the distance measurements, we find that majority (171) of the exoplanets are within the solar neighborhood ($\leq$300 pc). Relevant data related to the physical characteristics

Table 1. Number of planets with different exoplanetary detection missions.

Detection missions	No. of planets
CoRoT	14
HAT-P	09
HIP	03
HD catalog	125
Kepler	28
TrES	02
WASP	29
XO	01
Others	14

of planets and stars are presented in Table 2. As this exoplanetary catalog is a compilation of ground- and space-based observations, observers have used different statistical techniques for estimating the error bars in the physical and orbital characteristics of exoplanets. For example, hybrid Markov chain Monte Carlo (Gregory & Fischer 2010; Dumusque *et al.* 2014) and bootsrap (Barge *et al.* 2008) statistical method. However, basic errors that affect different physical parameters of the data are observational errors (Kovacs*et al.* 2010; Wakeford *et al.* 2013).

In Table 2, first two columns represent the name of an exoplanet and its mass in terms of Jupiter's mass. Third and fourth columns represent the semi-major axis and eccentricity respectively. The fifth and sixth columns represent the stellar metallicity [Fe/H] and stellar mass in terms of the solar mass. Whereas, the last column represents the stellar distance in parsec (pc).

3. Results and discussion

Before examining a relationship between the stellar (planetary) mass with stellar metallicity, let us examine how far the exoplanets are located in the solar neighborhood and, if any influence of average galactic metallicity on the stellar metallicity irrespective of galactic latitude and longitude. Figure 1(a) illustrates the distribution of planets with their distances from the Sun. The x-axis represents the distances of host stars from the Sun and y-axis represents the number of planets. Similarly, Fig. 1(b) illustrates the distribution of stellar metallicities with their distances from the Sun. It is obvious and not surprising from Fig. 1(a) that exponential decrease of number of planets with the distance is due to faintness of the observed stars. That means, with the present instruments, it is very difficult to precisely measure the radial velocity or transit curves of the exoplanets that are very far from the solar system. Hence, majority of exoplanets appear to occur within the solar neighborhood (≤ 300 pc). The Sun is situated in the galactic thin disk at about 20 pc above the galactic mid-plane. The gradient of radial variation of average metallicity in this galactic thin disk is 0.07 dex kpc^{-1} (Gonzalez *et al.* 2001a). It is interesting to check whether such a gradient of metallicity is also true if star's metallicity is influenced by galactic metallicity that in turn might have affected the planetary formation. In order to check this reasoning, irrespective of observed declinations (Dec.) and right ascensions (RA), we combine different metallicities and the same are plotted with respect to the observed stellar distances from the Sun. With the present data set, Fig. 1(b) illustrates the variation of stellar metallicity within the galactic thin disk. Since the majority of stars are within 300 pc, from the slope of Fig. 1(b) ($\sim$0.08 dex kpc^{-1}), one can say that variation of average galactic metallicity within the thin disk is negligible in the solar neighborhood. Of course, this is also evident from Fig. 2 wherein distribution of stars with metallicity for different galactic coordinates is illustrated. There appears to be concentration of metal-deficient stars (that have exoplanets) near both the galactic poles. Figure 1 and Fig. 2 show that observed exoplanetary systems are within the proximity ($\sim$2 kpc) of the Sun. Whereas, from 2–8 kpc, there is no observational evidence of detection of exoplanets. Unless we have information of observed exoplanetary systems from all parts of the galaxy, with the present dataset, it is difficult to conclude whether influence of galactic metallicity on the planetary formation exists or not.

3.1 *Stellar mass versus metallicity*

Previous studies (Winn & Fabrycky 2015 and references therein) show that metal-rich stars more likely harbor the planets. In addition, abundance of metallicity of stars with planets are more than the abundance of metallicity of stars without planets (Mortier *et al.* 2013). In these studies, results are obtained from an analysis of the host stars of all spectral types. However, it is interesting to know whether each spectral type, such as Sun-like G stars also follows the same trend or not. Importantly, it is essential to understand the behavior of stellar metallicity in both single and multiplanetary systems. In order to assert these ideas, in Fig. 3(a) and 3(b) we examine a relationship between stellar mass and stellar metallicity for all the planetary systems, irrespective of whether they are single or multiplanetary systems. In Fig. 3(a),

Table 2. Physical and orbital characteristics of the host stars and their exoplanets.

Name	M_p (M_J)	a (AU)	[Fe/H] (dex)	$M_\star$ ($M_\odot$)	Distance (pc)
47 Uma b	2.530(±0.065)	2.100	0(±0.07)	1.03(±0.050)	13.97
47 Uma c	0.540(±0.069)	3.600	0(±0.07)	1.03(±0.05)	13.97
47 Uma d	1.640(±0.385)	11.60	0(±0.07)	1.03(±0.050)	13.97
51 Peg b	0.468(±0.007)	0.052	0.2(±0.07)	1.11(±0.060)	14.70
61 Vir b	0.016(±0.001)	0.050	−0.01(±−)	0.95(±0.030)	8.52
61 Vir c	0.057(±0.003)	0.217	−0.01(±−)	0.95(±0.030)	8.52
61 Vir d	0.072(±0.008)	0.476	−0.01(±−)	0.95(±0.030)	8.52
70 Vir b	6.600(±0.660)	0.480	−0.11(±−)	0.92(±0.046)	22.00
CoRoT-1 b	1.030(±0.120)	0.025	0.06(±0.07)	0.95(±0.150)	460.00
CoRoT-12 b	0.917(±0.067)	0.040	0.16(±0.10)	1.07(±0.072)	1150.00
CoRoT-13 b	1.308(±0.066)	0.051	0.01(±0.07)	1.09(±0.020)	1310.00
CoRoT-16 b	0.535(±0.085)	0.061	0.19(±0.06)	1.09(±0.078)	840.00
CoRoT-17 b	2.430(±0.160)	0.046	0(±0.10)	1.04(±0.100)	920.00
CoRoT-18 b	3.470(±0.380)	0.029	−0.10(±0.10)	0.95(±0.150)	870.00
CoRoT-2 b	3.310(±0.160)	0.028	−0.04(±0.08)	0.97(±0.060)	300.00
CoRoT-20 b	4.240(±0.230)	0.090	0.14(±0.12)	1.14(±0.080)	1230.00
CoRoT-22 b	0.038(±0.035)	0.092	0.17(±0.09)	1.09(±0.049)	592.00
CoRoT-23 b	2.800(±0.250)	0.047	0.05(±0.10)	1.14(±0.080)	600.00
CoRoT-25 b	0.270(±0.040)	0.057	−0.01(±0.13)	1.09(±0.080)	1000
CoRoT-26 b	0.520(±0.050)	0.052	0.01(±0.13)	1.09(±0.060)	1670.00
CoRoT-27 b	10.390(±0.550)	0.047	0.10(±0.10)	1.05(±0.110)	–
CoRoT-9 b	0.840(±0.070)	0.407	−0.01(±0.006)	0.99(±0.040)	460.00
GJ 3021 b	3.370(±0.090)	0.490	0.10(±0.08)	0.90(±0.045)	17.62
HAT-P-1 b	0.525(±0.019)	0.055	0.13(±0.008)	1.15(±0.052)	139.00
HAT-P-15 b	1.946(±0.066)	0.096	0.22(±0.08)	1.01(±0.043)	190.00
HAT-P-21 b	4.063(±0.161)	0.049	0.01(±0.08)	0.94(±0.042)	254.00
HAT-P-22 b	2.147(±0.061)	0.041	0.24(±0.08)	0.91(±0.035)	82.00
HAT-P-23 b	2.090(±0.110)	0.023	0.16(±0.03)	1.13(±0.050)	393.00
HAT-P-25 b	0.567(±0.056)	0.046	0.31(±0.08)	1.01(±0.032)	297.00
HAT-P-27 b	0.660(±0.033)	0.040	0.29(±0.10)	0.94(±0.035)	204.00
HAT-P-28 b	0.626(±0.037)	0.043	0.12(±0.08)	1.02(±0.047)	395.00
HAT-P-38 b	0.267(±0.020)	0.052	0.06(±0.10)	0.88(±0.044)	249.00
HD 102117 b	0.172(±0.018)	0.153	0.30(±0.03)	1.03(±0.050)	42.00
HD 106252 b	7.560(±0.756)	2.700	−0.07	0.96(±0.048)	37.44
HD 106270 b	11.000(±0.800)	4.300	0.08(±0.03)	1.32(±0.092)	84.90
HD 10697 b	6.380(±0.530)	2.160	0.10(±0.06)	1.15(±0.030)	32.56
HD 108874 b	1.360(±0.130)	1.051	0.14	1.00(±0.050)	68.50
HD 108874 c	1.018(±0.300)	2.680	0.14	1.00(±0.050)	68.50
HD 109246 b	0.770(±0.090)	0.330	0.10	1.01(±0.110)	65.60
HD 114729 b	0.840(±0.084)	2.080	−0.22	0.93(±0.046)	35.00
HD 11506 b	3.440(±0.685)	2.430	0.31(±0.03)	1.19(±0.020)	53.82
HD 11506 c	0.820(±0.405)	0.639	0.31(±0.03)	1.19(±0.020)	53.82
HD 117207 b	2.060(±0.206)	3.780	0.27	1.07(±0.053)	33.00
HD 117618 b	0.178(±0.020)	0.176	0.04	1.05(±0.052)	38.00
HD 117618 c	0.200(±0.100)	0.930	0.04	1.05(±0.052)	38.00
HD 11964 b	0.622(±0.056)	3.160	0.17	1.12(±0.056)	33.98
HD 11964 c	0.079(±0.010)	0.229	0.17	1.12(±0.056)	33.98
HD 125612 b	3.000(±0.300)	1.370	0.24(±0.03)	1.10(±0.070)	52.82
HD 125612 c	0.058(±0.005)	0.050	0.24(±0.03)	1.10(±0.070)	52.82
HD 125612 d	7.200(±0.720)	4.200	0.24(±0.03)	1.10(±0.070)	52.82

Table 2. *Continued.*

Name	M_p (M_J)	a (AU)	[Fe/H] (dex)	$M_\star$ ($M_\odot$)	Distance (pc)
HD 12661 b	2.300(±0.230)	0.830	0.29(±0.05)	1.07(±0.053)	37.16
HD 12661 c	1.570(±0.157)	2.560	0.29(±0.05)	1.07(±0.053)	37.16
HD 134987 b	1.590(±0.020)	0.810	0.25(±0.02)	1.07(±0.080)	22.20
HD 134987 c	0.820(±0.030)	5.800	0.25(±0.02)	1.07(±0.080)	22.20
HD 136418 b	2.000(±0.100)	1.320	−0.07(±0.03)	1.33(±0.090)	98.20
HD 13931 b	1.880(±0.150)	5.150	0.03(±0.04)	1.02(±0.020)	44.20
HD 141937 b	9.700(±0.970)	1.520	0.11	1.10(±0.055)	33.46
HD 142 b	1.250(±0.150)	1.020	0.04(±0.05)	1.10(±0.220)	20.60
HD 142 c	5.300(±0.700)	6.800	0.04(±0.05)	1.10(±0.220)	20.60
HD 142415 b	1.620(±0.162)	1.050	0.21(±0.05)	1.09(±0.054)	34.20
HD 145377 b	5.760(±0.100)	0.450	0.12(±0.01)	1.12(±0.030)	57.70
HD 1461 b	0.023(±0.003)	0.063	0.19(±0.01)	1.08(±0.040)	23.40
HD 1461 c	0.018(±0.002)	0.111	0.19(±0.01)	1.08(±0.040)	23.40
HD 147513 b	1.210(±0.121)	1.320	−0.03	0.92(±0.046)	12.90
HD 149026 b	0.356(±0.012)	0.042	0.36(±0.05)	1.30(±0.100)	78.90
HD 150706 b	2.710(±0.900)	6.700	−0.13	0.94(±0.800)	27.20
HD 154672 b	5.020(±0.170)	0.600	0.26(±0.04)	1.06(±0.090)	65.80
HD 16141 b	0.215(±0.030)	0.350	0.02	1.01(±0.050)	35.90
HD 16175 b	4.400(±0.440)	2.100	0.23(±0.07)	1.35(±0.090)	59.80
HD 163607 b	0.770(±0.040)	0.360	0.21(±0.03)	1.09(±0.020)	69.00
HD 163607 c	2.290(±0.160)	2.420	0.21(±0.03)	1.09(±0.020)	69.00
HD 164509 b	0.480(±0.090)	0.875	0.21(±0.03)	1.13(±0.020)	52.00
HD 168443 b	7.659(±0.097)	0.293	0.04(±0.03)	0.99(±0.019)	37.38
HD 168746 b	0.230(±0.023)	0.065	−0.06(±0.05)	0.88(±0.010)	43.12
HD 170469 b	0.670(±0.067)	2.240	0.30(±0.03)	1.14(±0.020)	64.97
HD 171028 b	1.980(±0.198)	1.320	−0.49(±0.02)	0.99(±0.080)	90.00
HD 17156 b	3.191(±0.033)	0.162	0.24(±0.05)	1.27(±0.018)	78.24
HD 179079 b	0.080(±0.008)	0.110	0.29(±0.04)	1.08(±0.100)	63.69
HD 183263 b	3.670(±0.300)	1.510	0.30	1.17(±0.058)	53.00
HD 183263 c	3.820(±0.590)	4.250	0.30	1.17(±0.058)	53.00
HD 185269 b	0.940(±0.094)	0.077	0.11(±0.05)	1.28(±0.100)	47.00
HD 187123 b	0.520(±0.040)	0.042	0.16	1.06(±0.053)	50.00
HD 187123 c	1.990(±0.250)	4.890	0.16	1.06(±0.053)	50.00
HD 188015 b	1.260(±0.126)	1.190	0.29	1.09(±0.054)	52.60
HD 190360 b	1.502(±0.130)	3.920	0.24(±0.08)	1.04(±0.052)	15.89
HD 190360 c	0.057(±0.015)	0.128	0.24(±0.08)	1.04(±0.052)	15.89
HD 195019 b	3.700(±0.300)	0.138	0.08(±0.04)	1.06(±0.053)	18.77
HD 196050 b	2.830(±0.283)	2.470	0.23	1.17(±0.058)	46.90
HD 202206 c	2.440(±0.244)	2.550	0.37(±0.07)	1.13(±0.056)	46.34
HD 20367 b	1.070(±0.107)	1.250	0.10	1.04(±0.060)	27.00
HD 2039 b	4.900(±1.000)	2.200	0.10(±0.16)	0.98(±0.050)	89.80
HD 207832 b	0.560(±0.045)	0.570	0.06	0.94(±0.100)	54.40
HD 207832 c	0.730(±0.115)	2.112	0.06	0.94(±0.100)	54.40
HD 20794 b	0.008(±0.0009)	0.120	−0.38(±0.06)	0.85(±0.040)	6.06
HD 20794 c	0.007(±0.0013)	0.203	−0.38(±0.06)	0.85(±0.040)	6.06
HD 20794 d	0.015(±0.0019)	0.349	−0.38(±0.06)	0.85(±0.040)	6.06
HD 208487 b	0.413(±0.050)	0.510	−0.06(±0.05)	1.30(±0.065)	45.00
HD 209458 b	0.690(±0.017)	0.047	0.02(±0.05)	1.14(±0.022)	47.00
HD 210277 b	1.230(±0.030)	1.100	0.19(±0.04)	1.09(±0.054)	21.29
HD 212771 b	2.300(±0.400)	1.220	−0.21(±0.03)	1.15(±0.080)	131.00
HD 213240 b	4.500(±0.450)	2.030	0.16	1.22(±0.061)	40.75

Table 2. *Continued.*

Name	M_p (M_J)	a (AU)	[Fe/H] (dex)	$M_\star$ ($M_\odot$)	Distance (pc)
HD 216435 b	1.260(±0.130)	2.560	0.24	1.30	33.30
HD 216437 b	1.820(±0.182)	2.320	0.25	1.06(±0.053)	26.50
HD 217107 b	1.330(±0.050)	0.073	0.37(±0.05)	1.02(±0.051)	19.72
HD 217107 c	2.490(±0.250)	5.270	0.37(±0.05)	1.02(±0.051)	19.72
HD 219828 b	0.085(±0.008)	0.052	0.19(±0.03)	1.24(±0.062)	81.10
HD 222155 b	1.900(±0.600)	5.100	−0.11(±0.05)	1.13(±0.110)	49.10
HD 222582 b	7.750(±0.650)	1.350	−0.02	0.99(±0.049)	42.00
HD 224693 b	0.710(±0.071)	0.233	0.34(±0.03)	1.33(±0.100)	94.00
HD 28185 b	5.700(±0.570)	1.030	0.24	1.24(±0.062)	39.40
HD 28254 b	1.160(±0.080)	2.150	0.36(±0.03)	1.06(±0.053)	56.20
HD 290327 b	2.540(±0.155)	3.430	−0.11(±0.02)	0.90(±0.045)	54.90
HD 30177 b	7.700(±1.500)	2.600	0.19(±0.09)	0.95(±0.050)	55.00
HD 30669	0.470(±0.060)	2.690	0.13(±0.06)	0.92(±0.030)	57.00
HD 33283 b	0.330(±0.033)	0.168	0.36(±0.05)	1.24(±0.100)	86.00
HD 34445 b	0.790(±0.070)	2.070	0.14(±0.04)	1.07(±0.020)	46.50
HD 37124 b	0.675(±0.017)	0.533	−0.44	0.83(±0.041)	33.00
HD 37124 c	0.652(±0.052)	1.710	−0.44	0.83(±0.041)	33.00
HD 37124 d	0.696(±0.059)	2.807	−0.44	0.83(±0.041)	33.00
HD 38529 b	0.780(±0.078)	0.131	0.27(±0.05)	1.48(±0.050)	39.28
HD 39091 b	10.300(±1.030)	3.280	0.09	1.10(±0.055)	18.32
HD 4208 b	0.800(±0.080)	1.700	−0.28	0.87(±0.043)	33.90
HD 4308 b	0.040(±0.005)	0.118	−0.34	0.85(±0.042)	21.90
HD 44219 b	0.580(±0.050)	1.190	0.03(±0.01)	1.00(±0.050)	50.43
HD 45350 b	1.790(±0.140)	1.920	0.29	1.02(±0.051)	49.00
HD 49674 b	0.100(±0.010)	0.058	0.25	1.07(±0.053)	40.70
HD 50499 b	1.710(±0.200)	3.860	0.23	1.27(±0.063)	47.26
HD 52265 b	1.050(±0.030)	0.500	0.21(±0.06)	1.20(±0.060)	28.00
HD 52265 c	0.350(±0.090)	0.316	0.21(±0.06)	1.20(±0.060)	28.00
HD 564 b	0.330(±0.030)	1.200	0.13(±0.06)	0.92(±0.030)	54.00
HD 6434 b	0.390(±0.039)	0.140	−0.52	0.79(±0.039)	40.32
HD 6718 b	1.560(±0.105)	3.560	−0.06(±0.02)	0.96(±0.048)	55.90
HD 68988 b	1.900(±0.190)	0.071	0.24	1.20(±0.060)	58.00
HD 70642 b	2.000(±0.200)	3.300	0.16(±0.02)	1.00(±0.050)	28.80
HD 72659 b	3.150(±0.140)	4.740	−0.02(±0.01)	0.95(±2.000)	49.80
HD 73267 b	3.060(±0.070)	2.198	0.03(±0.02)	0.89(±0.030)	54.91
HD 73526 b	2.900(±0.200)	0.660	0.25(±0.05)	1.08(±0.050)	99.00
HD 73526 c	2.500(±0.300)	1.050	0.25(±0.05)	1.08(±0.050)	99.00
HD 73534 b	1.150(±0.115)	3.150	0.16(±0.04)	1.29(±0.100)	96.99
HD 74156 b	1.880(±0.030)	0.294	0.13	1.24(±0.040)	64.56
HD 74156 c	8.030(±0.120)	3.400	0.13	1.24(±0.040)	64.56
HD 75289 b	0.470(±0.047)	0.046	0.29	1.05(±0.052)	28.94
HD 75898 b	2.510(±0.251)	1.190	0.27(±0.05)	1.28(±0.130)	80.58
HD 76700 b	0.230(±0.023)	0.049	0.14	1(±0.050)	59.70
HD 81040 b	6.860(±0.710)	1.940	−0.16(±0.06)	0.96(±0.040)	32.56
HD 82886 b	1.300(±0.100)	1.650	−0.31(±0.03)	1.06(±0.074)	125.00
HD 82943 b	4.800(±0.480)	1.190	0.32	1.18(±0.059)	27.46
HD 82943 c	4.780(±0.478)	0.746	0.32	1.18(±0.059)	27.46
HD 82943 d	0.290(±0.031)	2.145	0.32	1.18(±0.059)	27.46
HD 8535 b	0.680(±0.055)	2.450	0.02	1.13(±0.056)	52.50
HD 88133 b	0.300(±0.030)	0.047	0.34(±0.04)	1.20(±0.200)	74.50

Table 2. *Continued.*

Name	M_p (M_J)	a (AU)	[Fe/H] (dex)	$M_\star$ ($M_\odot$)	Distance (pc)
HD 89307 b	2.000(±0.400)	3.340	−0.14(±0.04)	1.02(±0.040)	30.90
HD 92788 b	3.860(±0.386)	0.970	0.32	1.13(±0.056)	32.82
HD 92788 c	0.900(±0.300)	0.600	0.32	1.13(±0.056)	32.82
HD 9446 b	0.700(±0.060)	0.189	0.09(±0.05)	1.00(±0.100)	53.00
HD 9446 c	1.820(±0.170)	0.654	0.09(±0.05)	1.00(±0.100)	53.00
HD 96167 b	0.680(±0.180)	1.300	0.09(±0.05)	1.31(±0.090)	84.00
HIP 14810 b	3.880(±0.320)	0.069	0.26(±0.03)	0.99(±0.040)	52.90
HIP 14810 c	1.280(±0.100)	0.545	0.26(±0.03)	0.99(±0.040)	52.90
HIP 14810 d	0.570(±0.052)	1.890	0.26(±0.03)	0.99(±0.040)	52.90
HR 810 b	2.260(±0.180)	0.925	0.25	1.11(±0.070)	–
Kepler-10 b	0.010(±0.001)	0.016	−0.15(±0.04)	0.91(±0.021)	173.00
Kepler-10 c	0.054(±0.005)	0.241	−0.15(±0.04)	0.91(±0.021)	173.00
Kepler-11 b	0.005(±0.003)	0.091	0.0	0.95(±0.100)	–
Kepler-11 c	0.009(±0.007)	0.106	0.0	0.95(±0.100)	–
Kepler-11 d	0.022(±0.003)	0.159	0.0	0.95(±0.100)	–
Kepler-11 e	0.030(±0.005)	0.194	0.0	0.95(±0.100)	–
Kepler-11 f	0.006(±0.002)	0.250	0.0	0.95(±0.100)	–
Kepler-11 g	0.950(±0.475)	0.462	0.0	0.95(±0.100)	–
Kepler-12 b	0.431(±0.041)	0.055	0.07(±0.04)	1.16(±0.054)	–
Kepler-17 b	2.450(±0.014)	0.025	0.26(±0.10)	1.16(±0.060)	800
Kepler-20 b	0.026(±0.006)	0.045	0.02(±0.04)	0.91(±0.035)	290.00
Kepler-20 c	0.049(±0.007)	0.093	0.02(±0.04)	0.91(±0.035)	290.00
Kepler-20 d	0.060(±0.006)	0.345	0.02(±0.04)	0.91(±0.035)	290.00
Kepler-20 e	0.009(±0.0009)	0.050	0.02(±0.04)	0.91(±0.035)	290.00
Kepler-20 f	0.045(±0.004)	0.110	0.02(±0.04)	0.91(±0.035)	290.00
Kepler-22 b	0.110(±0.011)	0.849	−0.29(±0.06)	0.97(±0.060)	190.00
Kepler-4 b	0.082(±0.0128)	0.045	0.17(±0.06)	1.22(±0.091)	550.00
Kepler-41 b	0.490(±0.090)	0.029	−0.09(±0.16)	0.94(±0.090)	730.00
Kepler-412 b	0.939(±0.085)	0.029	0.27(±0.12)	1.16(±0.091)	1056.00
Kepler-43 b	3.230(±0.190)	0.044	0.33(±0.11)	1.32(±0.090)	1950.00
Kepler-44 b	1.020(±0.070)	0.045	0.26(±0.10)	1.19(±0.100)	2250.00
Kepler-66 b	0.310(±0.070)	0.135	0.01(±0.003)	1.03(±0.051)	1107.00
Kepler-67 b	0.310(±0.060)	0.117	0.01(±0.003)	0.86(±0.043)	1107.00
Kepler-75 b	9.900(±0.500)	0.080	−0.07(±0.15)	0.88(±0.060)	1140.00
Kepler-77 b	0.430(±0.032)	0.045	0.20(±0.05)	0.95(±0.040)	570.00
Kepler-78 b	0.005(±0.001)	0.010	−0.14(±0.08)	0.81(±0.050)	–
KOI-192 b	0.290(±0.090)	0.091	−0.19(±0.07)	0.96(±0.060)	1100.00
KOI-195 b	0.340(±0.080)	0.041	−0.21(±0.08)	0.91(±0.060)	880.00
mu Ara b	1.676(±0.167)	1.500	0.28(±0.04)	1.08(±0.050)	15.30
mu Ara c	0.033(±0.003)	0.090	0.28(±0.04)	1.08(±0.050)	15.30
mu Ara d	0.521(±0.052)	0.921	0.28(±0.04)	1.08(±0.050)	15.30
mu Ara e	1.814(±0.181)	5.235	0.28(±0.04)	1.08(±0.050)	15.30
TrES-2	1.253(±0.052)	0.035	−0.15(±0.10)	0.98(±0.062)	220.00
TrES-3	1.910(±0.065)	0.022	−0.19(±0.08)	0.92(±0.040)	–
WASP-104 b	1.272(±0.047)	0.029	0.32(±0.09)	1.02(±0.090)	143.00
WASP-110 b	0.515(±0.064)	0.045	−0.06(±0.10)	0.89(±0.072)	320.00
WASP-112 b	0.880(±0.120)	0.038	−0.64(±0.15)	0.80(±0.073)	450.00
WASP-12 b	1.404(±0.099)	0.022	0.30(±0.10)	1.35(±0.140)	427.00
WASP-16 b	0.855(±0.059)	0.042	0.01(±0.10)	1.02(±0.101)	–
WASP-19 b	1.114(±0.040)	0.016	0.02(±0.09)	0.90(±0.045)	–
WASP-21 b	0.300(±0.010)	0.052	−0.40(±0.10)	1.01(±0.025)	230.00

Table 2. *Continued.*

Name	M_p (M_J)	a (AU)	[Fe/H] (dex)	$M_\star$ ($M_\odot$)	Distance (pc)
WASP-25 b	0.580(±0.040)	0.047	−0.05(±0.10)	1.00(±0.030)	169.00
WASP-26 b	1.028(±0.021)	0.039	−0.02(0.09)	1.12(±0.030)	250.00
WASP-32 b	3.600(±0.070)	0.039	−0.13(±0.10)	1.10(±0.030)	–
WASP-34 b	0.590(±0.010)	0.052	−0.02(±0.10)	1.01(±0.070)	120.00
WASP-36 b	2.279(±0.068)	0.026	−0.31(±0.12)	1.02(±0.032)	450.00
WASP-37 b	1.800(±0.170)	0.043	−0.40(±0.12)	0.84(±0.040)	338.00
WASP-39 b	0.280(±0.030)	0.048	−0.12(±0.10)	0.93(±0.030)	230.00
WASP-4 b	1.237(±0.060)	0.023	−0.03(±0.09)	0.93(±0.050)	300.00
WASP-41 b	0.920(±0.070)	0.040	−0.08(±0.09)	0.95(±0.090)	180.00
WASP-44 b	0.889(±0.062)	0.034	0.06(±0.10)	0.95(±0.034)	–
WASP-46 b	2.101(±0.073)	0.024	−0.37(±0.13)	0.95(±0.034)	–
WASP-47 b	1.140(±0.050)	0.052	0.18(±0.07)	1.08(±0.370)	200.00
WASP-5 b	1.637(±0.082)	0.027	0.09(±0.09)	1.00(±0.060)	297.00
WASP-50 b	1.437(±0.068)	0.029	−0.12(±0.08)	0.86(±0.057)	230.00
WASP-58 b	0.890(±0.070)	0.056	−0.45(±0.09)	0.94(±0.100)	300.00
WASP-6 b	0.503(±0.028)	0.042	−0.20(±0.09)	0.88(±0.080)	307.00
WASP-63 b	0.380(±0.030)	0.057	0.08(±0.07)	1.32(±0.050)	330.00
WASP-8 b	2.244(±0.086)	0.080	0.17(±0.07)	1.03(±0.050)	87.00
WASP-95 b	1.130(±0.070)	0.034	0.14(±0.16)	1.11(±0.090)	–
WASP-96 b	0.480(±0.030)	0.045	0.14(±0.19)	1.06(±0.090)	–
WASP-97 b	1.320(±0.050)	0.033	0.23(±0.11)	1.12(±0.060)	–
WASP-98 b	0.830(±0.070)	0.036	−0.6(±0.19)	0.69(±0.060)	–
XO-5 b	1.077(±0.037)	0.048	0.18(±0.03)	0.88(±0.030)	–

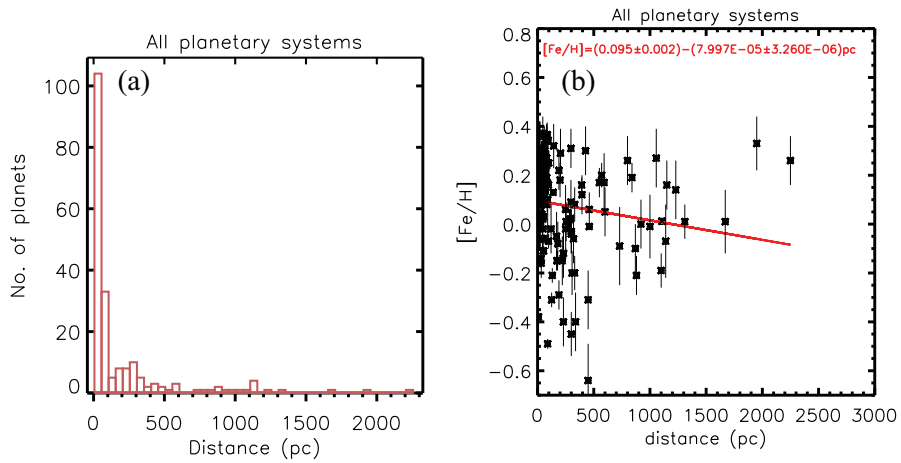

Figure 1. **(a)** The distribution of planets versus their host star's distance from the Solar system. In this figure, x-axis is binned with a size of 50 pc. **(b)** The dependency of observed stellar metallicity with the host star's distance from the Solar system for all planetary systems.

x-axis represents the observed metallicity with a bin size of 0.1 dex in which stellar masses are collected and, average and standard deviations (σ) are computed. Error in each bin is the estimated from the ratio $\frac{\sigma}{\sqrt{n}}$ (where n is the number of data points in each bin). Conventional usage is that, observed metallicity of a host star is a logarithmic value of ratio of star's [Fe/H] to Sun's [Fe/H]. In case, there is a linear relationship between host star's metallicity and different physical parameters of their respective host star and planets, then logarithmic values of metallicity have to be converted into absolute values. Now onwards this transformation from

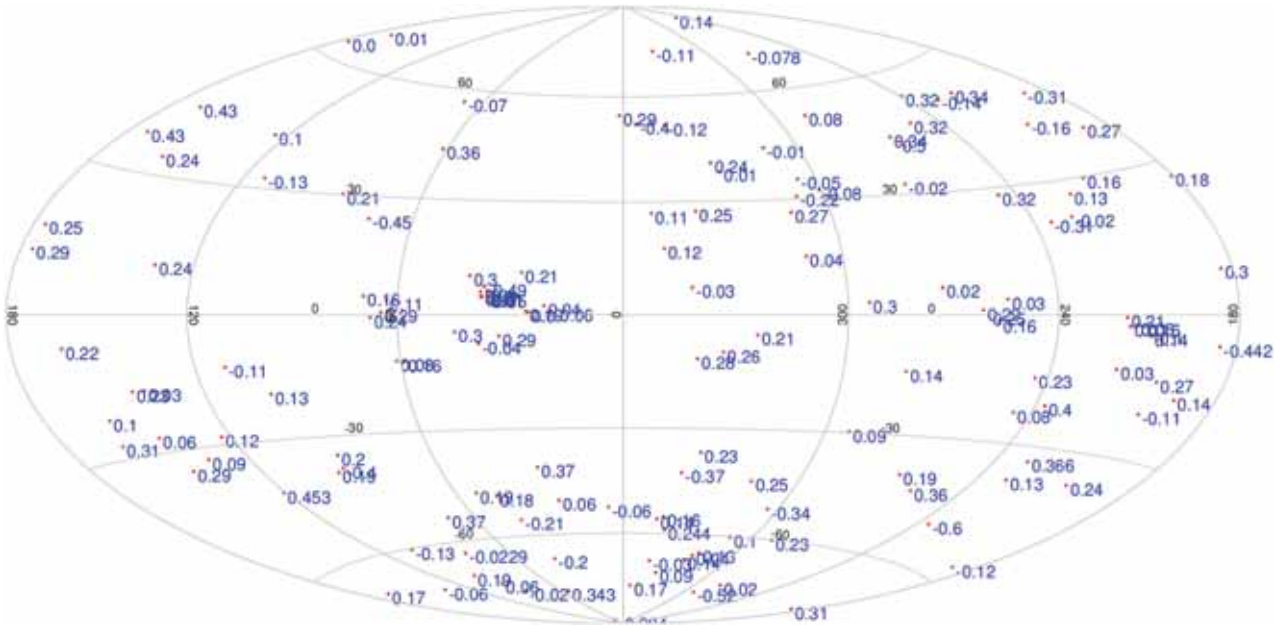

Figure 2. The distribution of stars (that harbor planets) with metallicity for different galactic coordinates within the observed distance of 2.1 kpc.

logarithmic scale to linear scale is called as *absolute metallicity* and is denoted as abs[Fe/H].

In Fig. 3(b), we illustrate a relationship between the stellar mass and absolute metallicity, where the absolute metallicity values are binned with a size of 0.25. The average and standard deviations σ of stellar masses in each bin are calculated as explained earlier. Errors in each bin are estimated from the ratio $\frac{\sigma}{\sqrt{n}}$.

Compared to a relationship between stellar mass and absolute metallicity (Fig. 3(b)), we find a strong relationship between logarithmic stellar mass and observed metallicity [Fe/H] (Fig. 3(a)) with a best fit of the following form:

$$\log\left(\frac{M_\star}{M_\odot}\right) = (0.007 \pm 0.006) + (0.165 \pm 0.026)[\text{Fe/H}], \quad (1)$$

where $M_\star$ is the stellar mass in terms of Sun's mass $M_\odot$. We conclude that a relationship illustrated in Fig. 3(a) is better than a relationship illustrated in Fig. 3(b) for the following reasons: (i) high correlation coefficient (99%) and (ii) small value of chi-square 1.376. Hence, it is concluded that there exists a power law relationship between the stellar mass and the observed metallicity.

One can notice from Fig. 3(a) that, the host star's metallicity increases non-linearly with increase in stellar mass. One can interpret this result as the metal rich stars are most likely originated in metal-rich disks. Due to high friction of dust and gas particles in a metal-rich nebula, the rate of formation of a central star (or accretion of mass on the central star) is much higher than the rate of formation (or accretion of mass on the central star) in a metal-poor nebula (Jones *et al.* 2016). The accretion process helps in acquiring more mass (i.e., more gas and dust particles that increases the chemical composition) by a central star. Hence, the metallicity of a host star is directly proportional to the stellar mass in logarithmic scale.

As explained in the Introduction, other plausible interpretation is that the accretion of disk or protoplanetary material or inward migration of planets add dust materials on the central star as a 'pollution' that ultimately increases the stellar metallicity. On the other hand, one can also argue that accretion of mass on a central star during later evolutionary stages may not increase the central mass substantially. Therefore, the effect of 'pollution' (accretion of mass) on the stellar mass is negligible, yet one can observe from Fig. 3(a) that metallicity increases as the stellar mass increase. Thus, one may conclude that contribution to the final stellar metallicity from 'pollution' is small and most of the stellar metallicity is likely to be of primordial composition of a nebula (Santos *et al.* 2004).

As the majority of stars in this analysis are single planetary systems, it is not clear whether multiplanetary systems follow a similar power law relationship. Thus, in order to delineate this combined data bias, in the following section, we investigate the stellar mass-metallicity relationship separately for single and

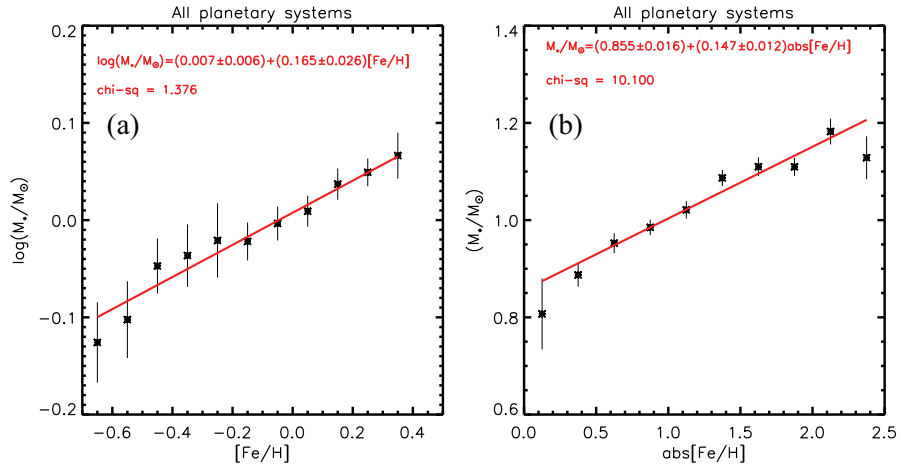

Figure 3. **(a)** The dependency of logarithmic stellar mass with the observed metallicity. The metallicity is binned with a size of 0.1 dex. **(b)** The dependency of stellar mass with the absolute metallicity for all planetary systems. The metallicity is binned with a size of 0.25. In both the figures, continuous line is a best least square fit between both the variables.

multiplanetary systems. Another aim of classification of this data is to examine whether single and multiplanetary systems originate in different ways or not. Hence, we investigate the relationship between stellar mass and metallicity for both single and multiplanetary systems in linear and non linear scales.

3.1.1 *Stellar mass versus metallicity: Multiplanetary systems*. In case of multiplanetary systems, Figures 4(a) and 4(b) show the variations of stellar mass with observed and absolute metallicity respectively, with the best fits as follows:

$$\frac{M_\star}{M_\odot} = (0.995 \pm 0.022) + (0.396 \pm 0.096)[\mathrm{Fe/H}] \quad (2)$$

and

$$\frac{M_\star}{M_\odot} = (0.801 \pm 0.012) + (0.161 \pm 0.022)\mathrm{abs}[\mathrm{Fe/H}]. \quad (3)$$

Among both the fits, if we accept χ^2 as a constraint on goodness of fit, stellar mass versus observed metallicity is a best fit (equation (2)). Both these relationships show a clear increasing trend between stellar mass and its metallicity. In Figures 4(a) and 4(b), the symbol $\odot$ represents metallicity of the Sun. One can notice from both the figures that the Sun's mass is slightly higher than the fitted line. This slight higher mass of the Sun might be due to 'pollution' from the solar system terrestrial planets. In other words, during the early history of the solar system formation, dust and gas materials in the vicinity of the Sun might have been accreted on the Sun (Melendez *et al.* 2009), that might have resulted in a slight increase in the Sun's mass. In case we accept this result, one can also estimate the amount of Sun's mass for the present metallicity, which is found to be $\sim 0.995 M_\odot$ from equation (2) and $\sim 0.962 M_\odot$ from equation (3). Hence, by accepting a value from a best fit (equation (2)), present mass of the Sun is about 1% higher than the original mass.

3.1.2 *Stellar mass versus metallicity: Single planetary systems*. Similar plots for single planetary systems are illustrated in Figures 4(c) and 4(d) respectively. In this case the best fit is obtained between the stellar mass and absolute metallicity, except that the stars that have same metallicity as those of multiplanetary systems produce massive planets. Hence, these results imply that the origin and formation of single and multiplanetary systems appear to be entirely different.

Coefficients of different linear and non linear laws that show the dependency of stellar mass on its metallicity are summarized in Table 3. The first column of Table 3 represents the different laws of fit, second and third columns represent the intercept (C1) and ratio of error in the intercept with respect to values of intercept ($|\frac{\delta C1}{C1}|$) respectively. The fourth and fifth columns represent the slope (C2) and the ratio of error in the slope with respect to values of slope ($|\frac{\delta C2}{C2}|$) respectively, followed by chi-square (a measure of goodness of fit) in the sixth column for all planetary systems. Similar results are presented in other columns that represent the single and multiplanetary systems respectively.

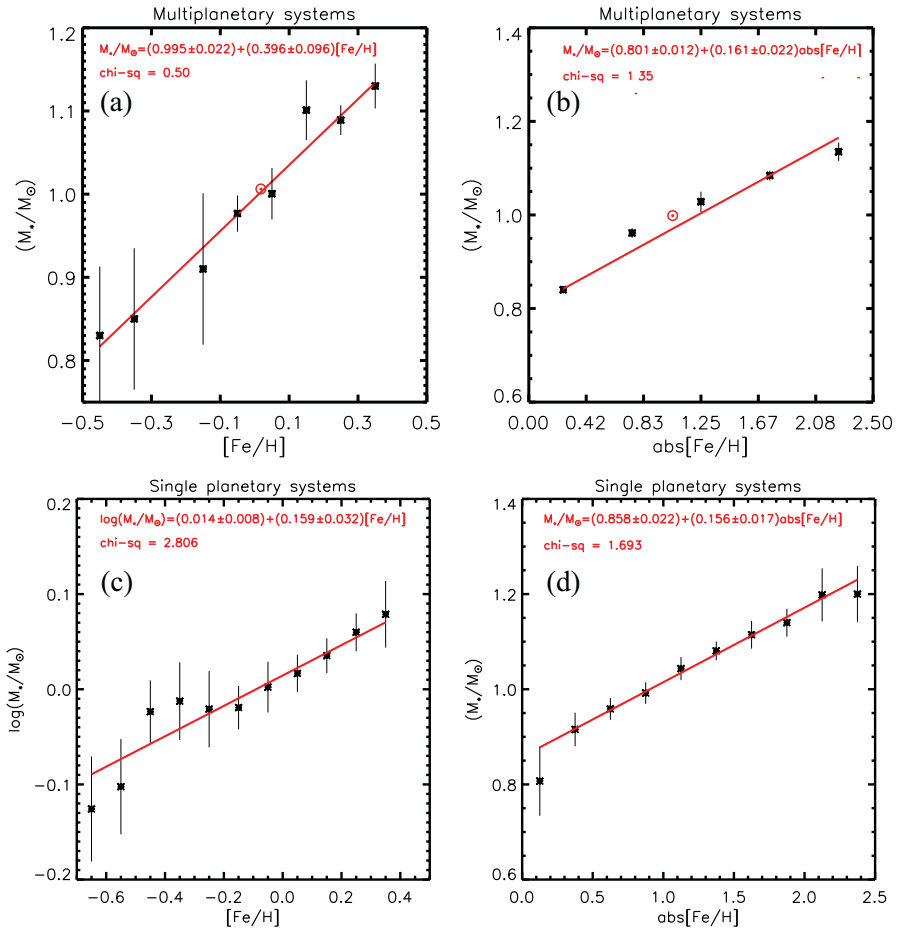

Figure 4. For multiplanetary systems, **(a)** and **(b)** illustrate the dependency of stellar mass with the observed and absolute metallicity respectively. For single planetary systems, **(c)** and **(d)** illustrate the dependency of stellar mass with the observed and absolute metallicity respectively. In all the plots, continuous line is a best least square fit. In (a) and (b), metallicity of the Sun is represented by ⊙.

Table 3. Stellar mass versus metallicity.

Different laws	All systems					Multiplanetary systems					Single planetary systems				
	C1	$\lvert\frac{\delta C1}{C1}\rvert$	C2	$\lvert\frac{\delta C2}{C2}\rvert$	χ^2	C1	$\lvert\frac{\delta C1}{C1}\rvert$	C2	$\lvert\frac{\delta C2}{C2}\rvert$	χ^2	C1	$\lvert\frac{\delta C1}{C1}\rvert$	C2	$\lvert\frac{\delta C2}{C2}\rvert$	χ^2
Linear–linear	0.855	0.018	0.147	0.081	10.100	0.801	0.014	0.161	0.136	1.35	0.858	0.025	0.156	0.108	1.693
Linear–log	1.021	0.005	0.377	0.066	7.831	0.995	0.022	0.396	0.242	0.50	1.036	0.007	0.370	0.083	14.878
Log–log	0.007	0.857	0.165	0.157	1.376	−0.003	7.333	0.173	0.578	0.10	0.014	0.571	0.159	0.201	2.806

3.2 *Dependence of metallicity with the planetary physical properties*

3.2.1 *Occurrence rates of single and multiplanetary systems*. In order to examine the occurrence rate of planets with metallicity, the number of planets in each bin is illustrated in Fig. 5 against the stellar metallicity for both observed and absolute values. One can notice from Figures 5(a) and 5(b) that the occurrence rates of planets are skewed Gaussian distributions with a peak around 0.0 to 0.2 dex in case of observed metallicity (Fig. 5(a)) and around 1.0 to 1.5 in case of absolute metallicity (Fig. 5(b)). For both Figures 5(a) and 5(b), best fits yield the lognormal and normal (Gaussian) distributions respectively. This apparent result strongly suggests that the occurrence rate of planets with stellar metallicity is a random phenomenon. This picture changes when we classify the data into two parts: (i)

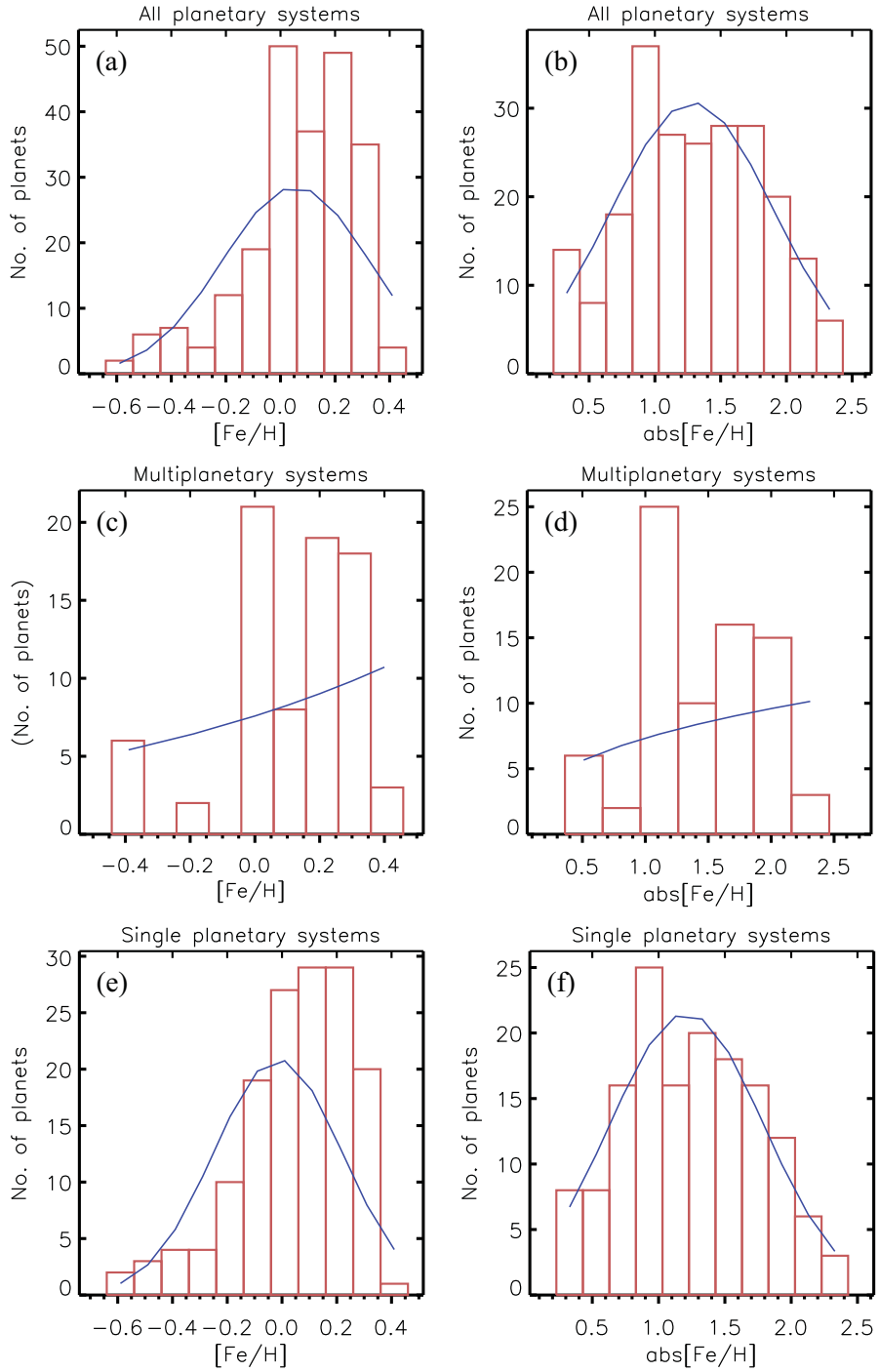

Figure 5. Histograms representation of number of the planets versus the stellar metallicity. **(a)** and **(b)** The dependency of the number of planets with the observed and absolute metallicity for all the planetary systems. **(c)** and **(d)** The dependency of the number of planets with the observed and absolute metallicity for the multiplanetary systems. **(e)** and **(f)** The dependency of the number of planets with the observed and absolute metallicity for the single planetary systems. The bin sizes are 0.1 dex and 0.2 in case of observed and absolute metallicity respectively.

multiplanetary systems and (ii) single planetary systems. As for multiplanetary systems, occurrence rate of planets with metallicity is not a random phenomenon, and we get a power-law relationship between both the variables. However, due to low statistics in the region of low metallicity ([Fe/H] < 0 or abs[Fe/H] < 1), with a caveat we conclude that more number of data-points are required to confirm an apparent power law

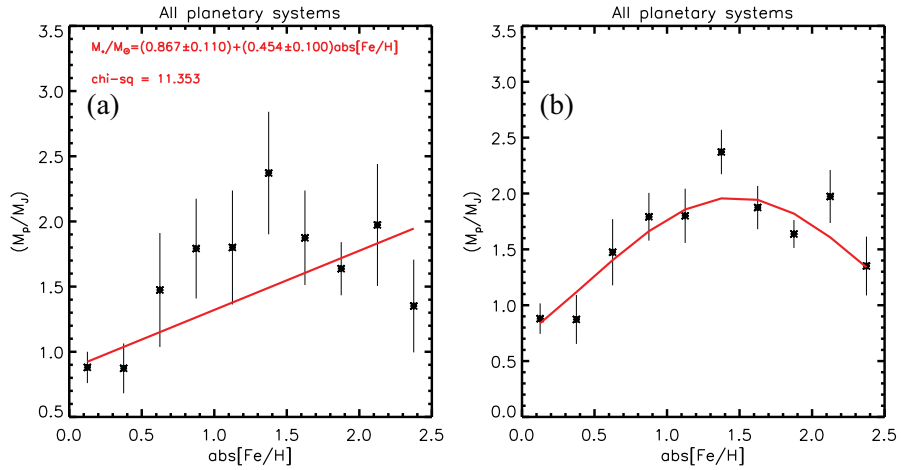

Figure 6. **(a)** The linear dependency of planetary mass with absolute stellar metallicity [Fe/H]. **(b)** The normal distribution of planetary mass with absolute metallicity. Both the plots are binned with a size of 0.25. In both the plots, continuous lines represent the best least square fits.

relationship between both the variables in case of multiplanetary systems. Whereas, single planetary systems follow lognormal and normal distributions as presented in Figures 5(e) and 5(f) respectively. From these two classifications it appears that single planetary systems probably might not have been originated from the host star's protoplanetary disk. This view will be strengthened from the results presented in the following sections 3.2.2 and 3.3.

3.2.2 *Planetary mass versus metallicity*. As mentioned earlier, chemical composition of nebula affects the planetary physical properties and metallicity of the host stars. Nayakshin (2015) showed that there is no correlation between the population of planets with metallicity except for gas giants that were present within few AU from the host star. In the present study we investigate the association between planetary mass with respect to stellar metallicity for single and multiplanetary systems. Probably this investigation may give hints on origin and formation of single and multiplanetary systems.

As metal-rich stars show the tendency of increased occurrence rate of planets, it is interesting to examine whether planetary mass is dependent on the stellar metallicity. In order to confirm this conjecture, in Fig. 6, irrespective of single and multiplanetary systems, we illustrate the dependence of planetary mass with respect to star's metallicity. The results presented in Fig. 6(a) show that, for absolute metallicity (linear–linear space), planetary mass is independent of host star's metallicity. Whereas in Fig. 6(b), a Gaussian or normal distribution fits very well for planetary mass–absolute metallicity relationship as follows:

$$\ln\left(\frac{M_{\rm p}}{M_{\rm J}}\right) = (-0.341 \pm 0.152) + (1.381 \pm 0.330)\text{abs[Fe/H]} - (0.469 \pm 0.142)\text{abs[Fe/H]}^2. \quad (4)$$

However, there is a data bias such that these fits are for the combined data set of single and multiplanetary systems. The data has been separated into single and multiplanetary systems in the following analysis.

Figure 7(a) represents the dependency of planetary mass with respect to stellar absolute metallicity in the case of multiplanetary systems. Whereas, in case of single planetary systems, Figures 7(b) and 7(c) illustrate the dependency of planetary mass with respect to the absolute metallicity with linear and normal distribution respectively. As illustrated in Fig. 7(a), although there is a scatter, variation of planetary mass clearly shows an increasing trend with the host star's absolute metallicity and best fit yields the following relationship

$$\frac{M_{\rm p}}{M_{\rm J}} = (0.861 \pm 0.740) + (1.363 \pm 0.429)\text{abs[Fe/H]}, \quad (5)$$

where $M_{\rm p}$ is the planetary mass in-terms of Jupiter mass $M_{\rm J}$.

Similarly, the relation between planetary mass and absolute metallicity for single planetary system (Fig. 7(c)) is given by the best fit of normal distribution as follows:

$$\ln\left(\frac{M_{\rm p}}{M_{\rm J}}\right) = (-0.426 \pm 0.154) + (2.240 \pm 0.366)\text{abs[Fe/H]} - (0.953 \pm 0.165)\text{abs[Fe/H]}^2. \quad (6)$$

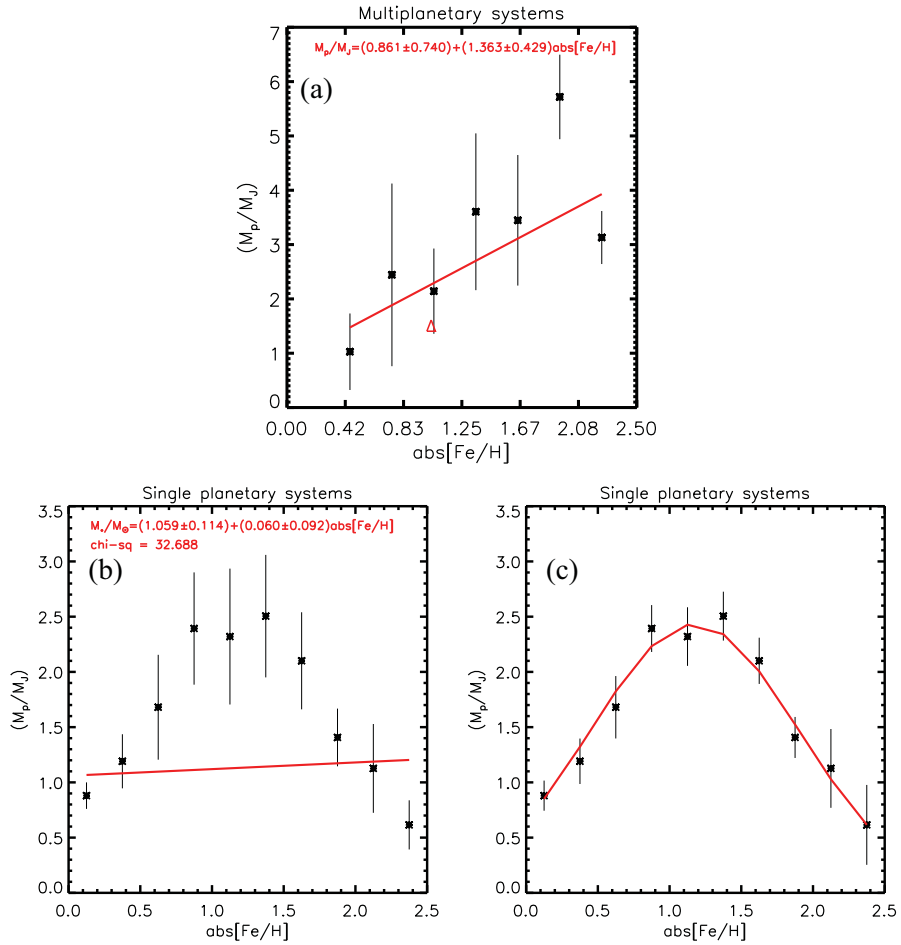

Figure 7. **(a)** For multiplanetary systems, the dependency of planetary mass with absolute metallicity, **(b)** for single planetary systems, the linear fit between planetary mass and absolute metallicity, and **(c)** the normal distribution. In all the plots, continuous line is a best least square fit. In (a), the total planetary mass of solar system is represented by a triangle.

Both these results suggest that, single planetary systems on average produce massive planets and probably their origin is different compared to multiplanetary systems.

As for the results presented in Fig. 7(a), following is the reason for low planetary mass for the metal-poor stars. Probably these metal-poor stars might have originated with metal-poor disks around them. These metal poor disks in turn might have less number of dust particles that eventually might have decreased the rate of planetary formation and hence less massive planets. Whereas in case of high metallicity stars with metal-rich disks, the scenario of planetary formation probably might be exactly opposite. Due to more number of gas and dust particles in the protoplanetary disk, time period of planet's core formation is less. Such a solid core rapidly acquires gas and dust particles as gaseous envelope to form massive or gas giants and grow big in size before dissipation of protoplanetary disk. Hence, the chance of formation of gas giants or massive planets is higher in case of metal rich stars.

3.2.3 *Estimation of solar system planetary mass*. With the equation (5) that relates planetary mass and stars metallicity for multiplanetary systems, it is interesting to examine whether total planetary mass of our solar system (a multiplanetary system) follows such a universal relationship. We find that the estimated total planetary mass of the solar system, by using equation (5), is $\sim$2.224 M_J which is roughly 1.5 times higher compared to the present observed solar system total mass ($\sim$1.4 M_J) (that includes masses of asteroids, Kuiper belt and Oort's cloud objects). This result suggests that there is a missing mass of $\sim$0.8 M_J in the solar system planetary bodies. Let us conjecture where this missing mass of $\sim$0.8 M_J might have gone. When we closely examine Fig. 3(a), a decrease of about 1% mass from the present solar mass fits the universal law of stellar mass-metallicity relationship. One possibility is that such a

missing planetary mass might have accreted onto the Sun during the early history of the solar system formation (Melendez *et al.* 2009). However, at present it is not clear how much percentage of missing mass ($\sim 0.8 M_{\rm J}$) is accreted onto the Sun. Moreover, due to high activity of the Sun during the early history of solar system formation, some parts of planetary missing mass in the vicinity of the Sun might have also been blown off to the outer region probably through ambient magnetic field lines. The leftover dust particles within the vicinity of the Sun might have formed as terrestrial planets. Hence, due to less amount of gas and dust particles, the inner planets were unable to grow bigger in size explaining why solar terrestrial planets are less massive compared to Jovian planets. In fact in the previous study (Shashanka *et al.* 2015), we came to a similar conclusion.

3.2.4 *Estimation of planetary mass beyond the solar system Kuiper belt*. Coming to the picture of missing mass, if protoplanetary disk is in hydrostatic equilibrium, then density ρ varies as $\rho_0 e^{\frac{-r}{H}}$ (where ρ_0 is density at the center, r is distance from the center and, H is density scale height), where maximum density is concentrated near the center. In case we accept this reasonable density profile, then there is every possibility that maximum missing mass (∼80%) might be accreted onto the Sun. Whereas a small (∼20%) mass that is in plasma state might have been transported along the magnetic field lines to larger distances, probably beyond the present Kuiper belt objects. That means, about 20% of missing mass might have been dumped into the outer regions of the solar system. Interestingly, this 20% of missing mass turns out to be ∼60 Earth's mass that is probably residing in the outer edge of the solar system unless it is ejected from the catastrophic events. In fact, this interesting estimation of missing mass might have formed as ninth and tenth or probably more planets in the outer region (∼200 AU) of the solar system (Batygin & Brown 2016).

3.2.5 *Single planetary systems: Wandering and captured planets*. When we examine the results emerged from the histograms (Figures 5(a), 5(b), 5(e) and 5(f)), and planetary mass–stellar metallicity relationships (Figures 6(b) and 7(c)), events are random and there is no relationship between metallicity of the host stars and planets of the single planetary systems. That means, these planets probably are not formed in the host star's protoplanetary disks. Rather these planets might have been originated and were formed elsewhere in the galaxy, wandered and probably captured by the host stars. One can notice that single planetary systems are majority in the present data set. However, with a power-law, Figures 5(c) and 5(d) confirm that planets in the multiplanetary systems are not random events. That means, these planets are not captured from the space, instead most likely they are originated in the protoplanetary disks around the host stars.

3.3 *Orbital distances of exoplanets versus stellar metallicity*

Planets prefer to form in the cooler region of protoplanetary disk. This is because, at high temperature, the rate of condensation of gas and dust particles is low due to high activity of the central star, like Sun (Hiremath 2009). Hence most of the planets migrate before settling into the stable orbits around their host stars. Inspite of migration of the planets, it is interesting to examine whether orbital distances of planets depend upon the metallicity of the host stars. Figure 8(a) illustrates the variation of average orbital distances for all the planets versus absolute metallicity with a bin size of 0.1 dex. Whereas, Fig. 8(b) represents the same relationship for single planetary systems. One can notice that among all the fits (linear–linear, log–log and lognormal distribution space), for the both the figures, lognormal distribution is a best fit with the following forms:

$$\begin{aligned}\ln(a) = {} & (0.533 \pm 0.112) \\ & + (0.407 \pm 0.346)[\text{Fe/H}] \\ & - (8.406 \pm 0.708)[\text{Fe/H}]^2, \end{aligned} \tag{7}$$

and

$$\begin{aligned}\ln(a) = {} & (0.386 \pm 0.122) - (0.639 \pm 0.455)[\text{Fe/H}] \\ & - (9.678 \pm 0.839)[\text{Fe/H}]^2. \end{aligned} \tag{8}$$

These relationships suggest that, occurrence events of single planetary systems are random. Hence, as we discussed in section 3.2.5, again an inevitable conclusion is that single planetary systems most likely are captured planets from space.

For multiplanetary systems, Fig. 8(c) illustrates the stable orbital distances of the planets as a function of absolute metallicity that clearly suggests a direct relationship. Careful observation of Figures 8(b) and 8(c) reveals that average semi major axis of stable orbits for the multiplanetary systems (Fig. 8(c)) is higher than the average semi major axis for single planetary systems (Fig. 8(b)). Hence, these results show that inward migration of planets and probably accretion of planetary mass on to the host stars is dominant in case of single planetary systems. This accretion of planetary

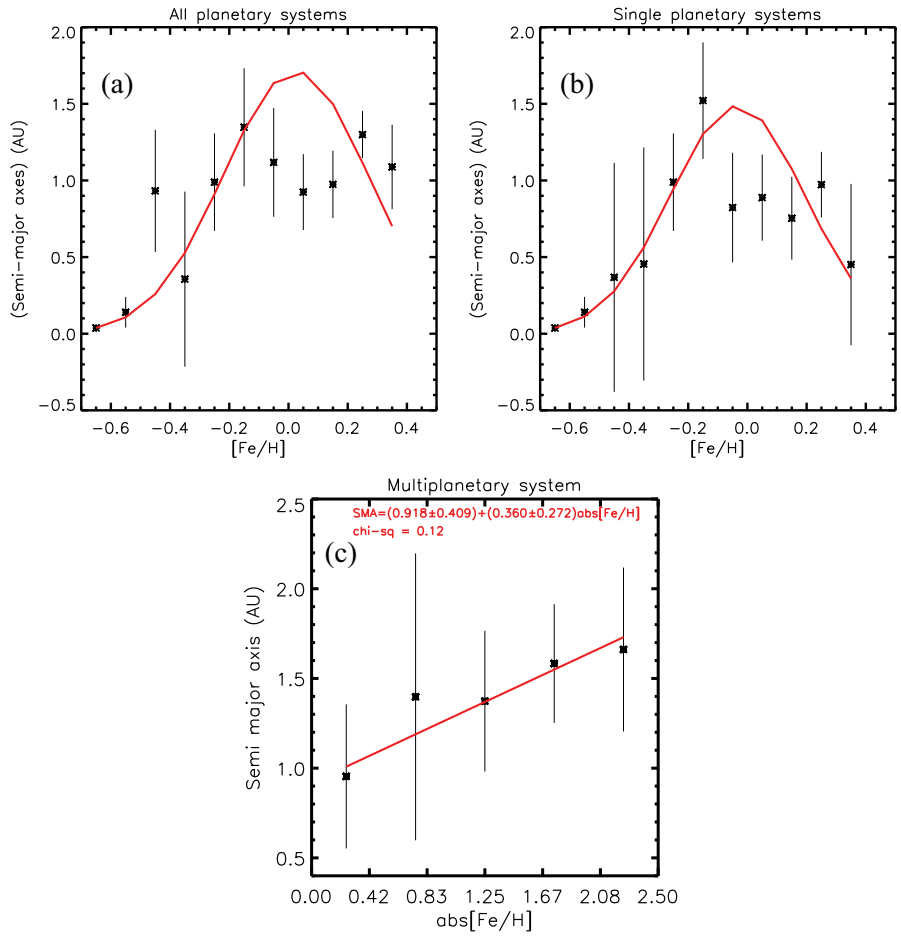

Figure 8. **(a)** and **(b)** illustrate the lognormal distribution of semi major axis with the observed metallicity for all planetary systems and single planetary systems respectively. **(c)** illustrates the dependency of semi-major axis of planets with the absolute metallicity for multiplanetary systems. In case of multiplanetary systems, metallicity is binned with a size of 0.5, whereas in case of all and single planetary system, it is 0.1 dex.

mass on the central host star acts as a 'pollution' and further increases the stellar metallicity. As for multiplanetary systems, it appears that inward migration is less compared to migration in case of single planetary systems.

4. Conclusions

To conclude this study, we have considered the physical characteristics of Sun-like G stars and their exoplanets with their orbital distances. Initially, an analysis has been done to examine the effect of galactic metallicity on the planetary formation. However, we conclude that with the present dataset of Sun-like stars, it is difficult to infer the influence of galactic metallicity on the stellar/planetary system formation. Further, the association between stellar mass with their metallicity is examined. We find that, there is a direct relationship between the logarithmic stellar mass and its metallicity that suggests most of the stellar metallicity is due to primordial origin. Hence, the contribution of 'pollution' to the final stellar metallicity is small.

The investigation of planetary mass with respect to their stellar absolute metallicity for all planetary systems, does not show any significant dependence on each other. However, an analysis by separating the dataset into single and multiplanetary systems reveals that, in case of multiplanetary systems, planetary mass is linearly dependent on the stellar absolute metallicity. Whereas, we find a normal distribution between the same variables in case of single planetary systems, that suggests most of the planets in single planetary systems might be captured from space.

Interestingly, the relationship between planetary mass and absolute metallicity for multiplanetary systems suggests that there is a missing planetary mass ($\sim 0.8 M_{\rm J}$) in the solar system. It is argued that majority ($\sim$80%)

of the missing planetary mass might have been accreted onto the Sun and a small fraction (∼20%) might have been blown off to the outer part of the solar system during early evolutionary stage. This 20% of the missing mass is estimated to be ∼60 Earth mass that probably resides beyond the Kuiper′s belt of the solar system.

Finally, a study of dependency of orbital distance on absolute stellar metallicity reveals that both these variables are linearly dependent on each other in case of multiplanetary systems. Whereas, in case of single planetary systems, lognormal distribution fits very well between orbital distance and observed stellar metallicity suggesting that, inward migration of the planets is dominant in case of single planetary systems during the early stages of orbital evolution.

Acknowledgements

The authors are grateful to the referee for invaluable comments that resulted in substantial improvement of the manuscript. The first author is thankful to Ms. N. Sindhu of VIT University, Vellore for preparing Fig. 2.

References

Adibekyan, V. Zh., Santos, N. C., Sousa, S. G. *et al.* 2012, *A&A*, **543**, A89.
Antoniadou, K. I., Voyatzis, G. 2016, *MNRAS*, **461**, 3822.
Barge, P., Baglin, A., Auvergne, M. *et al.* 2008, *A&A*, **482**, L17
Batygin, K., Brown, M. E. 2016, *AJ*, **151**, 22.
Bean, J. L., Benedict, G. F., Endl, M. 2006, *ApJ*, **653**, L65.
Boss, A. P., Hudgins, D. M., Traub, W. A. 2010, Proceedings IAU Symposium No. 276.
Bodaghee, A., Santos, N. C., Israelian, G., Mayor, M. 2003, *A&A*, **404**, 715.
Brugamyer, E., Dodson-Robinson, S. E., Cochran, W. D. *et al.* 2011, *ApJ*, **738**, 97.
Buchhave, L. A., Bizzarro, M., Latham, D. W. *et al.* 2014, *Nature*, **509**, 593.
Da Silva, R., Milone, A. C., Reddy, B. E. 2011, *A&A*, **526**, A71.
Dawson, R. I., Murray-Clay, R. A. 2013, *ApJL*, **767**, L24.
Dressing, C. D., Charbonneau, D. 2015, *ApJ*, **807**, 23.
Dumusque, X., Bonomo, A. S., Haywood, R. D. *et al.* 2014, *ApJ*, **789**, 154.
de Wit, J., Seager, S. 2013, *Science*, **342**, 1473.
Fischer, D., Valenti, J. 2005, *ApJ*, **622**, 1102.
Gonzalez, G. 2000, *ASP Conference series*, **219**, 523.
Gonzalez, G. 2003, *ASP Conference series*, **294**, 129.
Gonzalez, G. 2006, *PASP*, **118**, 1494.
Gonzalez, G., Donald, B., Ward, P. 2001a, *Icarus*, **152**, 185.
Gonzalez, G. Laws, C., Tyagi, S. *et al.* 2001b, *AJ*, **121**, 432.
Gregory, P. C., Fischer, D. A. 2010, *MNRAS*, **403**, 731.
Hiremath, K. M. 2009, *Sun & Geosphere*, **4**, 16.
Jones, M. I., Jenkins, J. S., Brahm, R. *et al.* 2016, *A&A*, **590**, A38.
Kerr, M., Johnston, S., Hobbs, G. *et al.* 2015, *ApJL*, **809**, L11.
Kovacs, G., Bakos, G. A., Hartman, J. D. *et al.* 2010, *ApJ*, **724**, 866.
Ksanfomality, L. V. 2004, *Solar System Research*, **38**(5), 372.
Lammer, H., Dvorak, R., Deleuil, M. *et al.* 2010, *Solar System Research*, **44**(6), 520.
Lindgren, S., Heiter, U., Seifahrt, A., 2016, *A&A*, **586**, A100.
Maldonado, J., Villaver, E., Eiroa, C. 2013, *A&A*, **554**, A84.
Melendez, J., Asplund, M., Gustafsson, B., Yong, D. 2009, *ApJ*, **704**, L66.
Mena, E. D., Israelian, G., Hernandez, J. I. G. *et al.* 2012, *ApJ*, **746**, 47.
Mordasini, C., Alibert, Y., Benz, W. *et al.* 2012, *A&A*, **541**, A97.
Moriarty, J., Madhusudhan, N., Fischer, D. A. 2014, *ApJ*, **787**, 81.
Mortier, A., Santos, N. C., Sousa, S. G. *et al.* 2013, *A&A*, **557**, A70.
Nayakshin, S. V. 2015, *BAAS*, **47**, 6.
Reboussin, L., Wakelam, V., Guilloteau, S. *et al.* 2015, *A&A*, **579**, A82.
Reddy, B. E., Lambert, D. L., Laws, C. *et al.* 2002, *MNRAS*, **335**, 1005.
Santos, N. C., Israelian, G., Lopez, R. J. G. *et al.* 2004, *A&A*, **427**, 1085.
Santos, N. C., Israelian, G., Mayor, M. 2000, *A&A*, **363**, 228.
Santos, N. C., Mena, E. D., Israelian, G. *et al.* 2009, *Proc. IAU Sympoium*, **268**, 291.
Shashanka, R. G., Hiremath, K. M., Ramasubramanian, V. 2015, submitted to *MNRAS*
Vauclair, S., Vauclair, G. 2014, *SF2A*, 285.
Wakeford, H. R., Sing, D. K., Deming, D. *et al.* 2013, *MNRAS*, **435**, 3481.
Walsh, C., Millar, T, J̃. 2011, *IAU Symposium*, **280**, 56.
Wang, J., Fischer, D. A. 2015, *AJ*, **149**, 14.
Winn, J. N., Fabrycky, D. C. 2015, *Annu. Rev. Astron. Astrophys.*, **53**, 409.